ISBN: 978-3-95450-261-5 ISSN: 2673-7000 doi: 10.18429/JACoW-NAPAC2025-WECN01

LCLS-II INJECTOR OPERATIONAL CHALLENGES AND RECENT DEVELOPMENTS*

F. Zhou†, A. Brachmann, D. Cesar, W. Colocho, Y. Ding, D. Dowell, G. Just, A. Osman, N. Sudar, J. Tang, T. Vecchione, Z. Zhang, C. Zimmer
SLAC National Accelerator Laboratory, Menlo Park, CA, USA

Abstract

The Linac Coherent Light Source II (LCLS-II) has been in user operations since 2023 and has successfully ramped up the beam repetition rate to 93 kHz. The LCLS-II photoinjector has demonstrated the ability to deliver a high-brightness, low-emittance electron beam at high repetition rates, meeting key performance targets. However, several operational challenges have emerged during commissioning and user operation. These include substantial gun dark current, degradation of cathode quantum efficiency (QE) manifesting as QE craters, unexpected electron beam splitting, significant emittance growth through the laser heater chicane, complications during laser heater commissioning, and the presence of beam halos. This paper provides an overview of these challenges and highlights recent efforts to address these outstanding issues.

INTRODUCTION

Continuous-wave (CW) free-electron laser (FEL) facilities such as LCLS-II impose stringent requirements on the photoinjector to deliver high-brightness, low-emittance, and reliable electron beams. The LCLS-II 1 MeV electron source was successfully commissioned between 2018 and 2020, following the resolution of several significant technical challenges [1]. In 2022, the full-scale >70 MeV injector was commissioned, and its beam performance was then characterized and optimized. Figure 1 presents a schematic layout of the complete injector system.

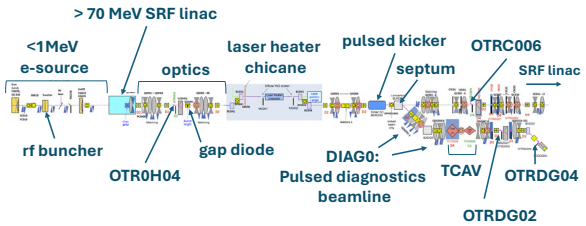

Figure 1: Schematic of the LCLS-II injector layout.

The injector consists of the 1 MeV electron source, a >70 MeV standard cryomodule (CM01), a laser heater chicane, and multiple diagnostic stations. These include the first emittance station (OTR0H04) and a gap diode for relative bunch length measurements, both located before the laser heater chicane; a second emittance station (OTRC006) located downstream of the chicane; and a dedicated off-axis diagnostics station equipped with a transverse deflecting cavity (TCAV) for absolute bunch length measurement, along with an additional emittance measurement station.

Since the start of FEL user operations in 2023, a variety of operational challenges have been encountered in the injector system. This paper discusses the key issues and the corresponding efforts toward their resolutions, including:

- A steady gun vacuum pressure rise over the time.
- Large gun dark current, which has led to frequent damages to downstream camera electronics, formation of localized hot spots, and beam loss events that trigger full machine trips.
- The formation of quantum efficiency (QE) crater on the photocathode after just a few days of operation, resulting in spatial and charge instability in the beam.
- Nonlinear magnetic fields in the laser heater chicane, contributing to significant emittance growth.
- Lessons learned from commissioning the laser heater.
- The presence and mitigation of beam halos.

OPERATIONAL CHALLENGES AND RECENT DEVELOPMENTS

The following sub-sections present an overview of each operational challenge and the systematic efforts undertaken to diagnose and resolve them.

CW Gun Operational Improvement

Figure 2 shows the gun vacuum gradually degraded over time, increasing from 8×10^{-10} Torr in 2023 to 2×10^{-9} Torr by 2024. In October 2024, a small step-like increase in vacuum pressure was observed; however, the source of this change remained unidentified until December 2024, when a vacuum leak was discovered on one of two RF windows. Following the identification of the leak, the faulty window was replaced, and the entire gun assembly was baked at 150–170 °C.

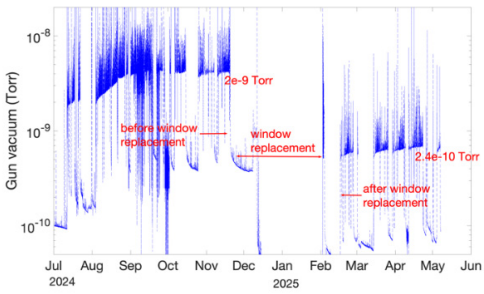

Figure 2: Gun vacuum trends before and after gun window replacement.

Historically, during RF power processing of the gun, we would 'jump' over the multipacting barriers by rapidly

* Work supported by DOE contract # DE-AC02-76SF00515
† zhoufeng@slac.stanford.edu

ISBN: 978-3-95450-261-5 ISSN: 2673-7000 doi: 10.18429/JACoW-NAPAC2025-WECN01

increasing the RF power. However, during processing with the replaced window all multipacting barriers were fully processed through, resulting in a significant improvement in vacuum conditions. The base pressure with CW RF on was improved by a factor of 10. In addition, over the past five months following RF processing, the gun vacuum has remained stable at 2.4×10^{-10} Torr. Figure 2 illustrates the gun vacuum trend before and after the RF window replacement.

Gun Dark Current Mitigations

The CW normal-conducting RF gun generates several μA of dark current, primarily originating from localized emission sites near the rim of the 10 mm-diameter cathode plug. This dark current presents a significant risk to the permanent magnets in the undulator sections due to potential radiation-induced damage. To mitigate this risk, a circular collimator was initially installed to intercept the dark current at low energies (<1 MeV), thereby reducing radiation production. The collimator, with a 20 mm aperture, effectively blocks approximately 90% of the dark current, resulting in a manageable power loss of only 1–2 W and negligible impact on the photo-injected beam. However, the remaining ~10% of dark current is accelerated through the cryomodules, still causing beam losses at various downstream locations. These losses have led to frequent damage to camera systems and laser energy meter electronics, the formation of localized hot spots, and beam loss events that trigger full machine trips.

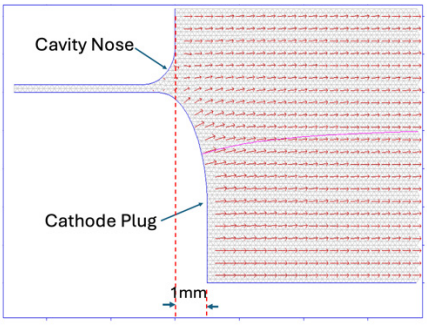

Figure 3: Electric field profile of the 1-mm over-inserted cathode [2].

In 2024, a 1-mm over-inserted cathode was developed [2], as illustrated in Fig. 3, to reduce the dark current propagating downstream through the beamline. This design lowers the electric field gradient at the nose of the cavity, which has been identified as the primary source of gun dark current. Additionally, the increased defocusing effect helps steer the dark current away from the cathode axis, significantly reducing the amount transported through the first cryomodule. At the same time, the modified geometry enhances the electric field gradient at the cathode surface, which may improve beam emittance. The over-inserted cathode was deployed at the LCLS-II injector on February 25, 2025, leading to a dark current reduction of more than 1000-fold, as shown in Fig. 4. This dramatic improvement has substantially enhanced machine availability and beam quality.

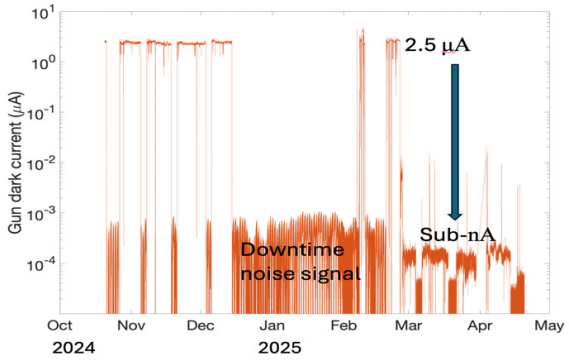

Figure 4: Log of the gun dark current vs. months with standard flat cathode, and over-inserted cathode beginning Feb 25, 2025.

Cathode's QE Uniformity Evolution

Cs_2Te cathodes grown at SLAC have been used for LCLS-II operations. It was observed that all standard flat cathodes developed quantum efficiency (QE) craters, as shown in the top row of plots in Fig. 5, after only a few days of operation - even at low beam repetition rates, such as 10 Hz. The formation of these QE craters is attributed to ion back-bombardment, primarily driven by the high gun dark current near the cathode surface. The presence of a QE crater leads to beam pointing instability and emittance degradation due to increased QE non-uniformity.

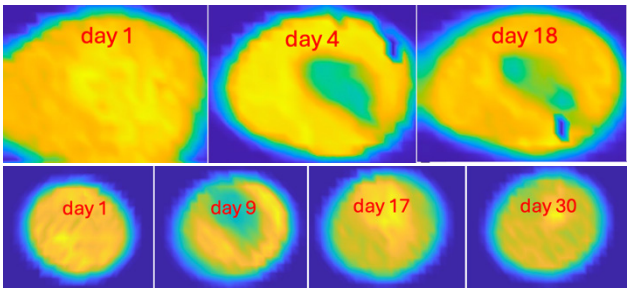

Figure 5: QE uniformity evolution over time: with standard flat cathode (top row) and with over-inserted cathode (bottom row). Cs_2Te area is approximately 3.5 mm in diameter. Laser size on the cathode is 0.8mm diameter.

Since February 2025, over-inserted cathodes have been adopted for routine operations. With this new design, the evolution of QE craters has significantly slowed down, and QE uniformity recovers more quickly after initial degradation, as demonstrated in the bottom row of Fig. 5. We attribute this improvement to the substantial reduction in gun dark current, which greatly limits ion generation near the cathode surface and thereby mitigates QE damage.

Nonlinear Field Correction for Emittance Preservation

A normalized emittance of 0.5 μm is routinely achieved at the first injector emittance station (OTR0H04). However, significant emittance growth, by a factor of 2 to 3, was consistently observed at the second injector emittance station (OTRC006), located downstream of the laser heater chicane. Figure 6 shows measured emittances at the first (top

ISBN: 978-3-95450-261-5 ISSN: 2673-7000 doi: 10.18429/JACoW-NAPAC2025-WECN01

left) and second (top right) emittance stations, where a typical doubling of emittance is evident after the beam passes through the chicane. Additionally, achieving consistent beam optics matching at the second station was found to be challenging.

To investigate the cause of this emittance growth, a series of systematic studies were conducted. These investigations ultimately revealed that low-carbon steel plates had been used to support lead shielding near the second bend of the laser heater chicane. Electromagnetic modeling indicated that these steel supports introduced magnetic field perturbations of 1–3% for the second dipole, which distorted the beam optics and contributed to emittance degradation. To correct this, the low-carbon steel was replaced with non-magnetic stainless steel in the shielding support structures. Following this modification, emittance preservation through the chicane improved significantly, and beam optics matching at the second station became consistently reliable. Figure 6 includes a comparison of emittance measurements taken before (top) and after (bottom) the replacement, demonstrating the effectiveness of this correction.

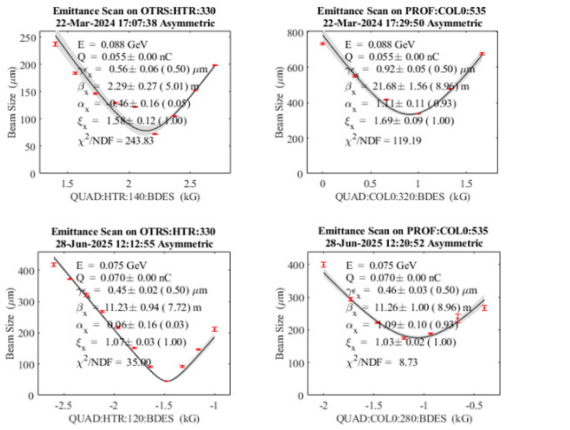

Figure 6: Emittance before (top) and after (bottom) correction of the low carbon steel at the 1st (left) and 2nd (right) emittance stations.

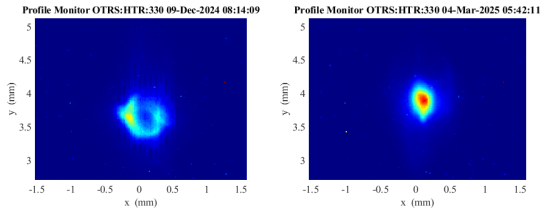

Figure 7: e-beam shape with smaller (left) and larger (right) laser sizes.

Beam Split and Solution

A split or donut-shaped beam profile was frequently observed on both injector screens, as shown in Fig. 7 (left) as an example. This beam deformation had a direct and detrimental impact on FEL performance. Systematic modeling identified space charge effects due to the small size of the drive laser spot on the cathode—as the primary cause of the observed beam distortion. To address this issue, the laser size diameter was increased from 0.65 mm to 0.8 mm. With proper solenoid field, the split beam structure was eliminated, as shown in Fig. 7 (right) without compromising beam emittance.

Laser Heater Commissioning Lessons

Despite more than six months of intensive effort, no energy modulation was observed from the laser heater undulator. Several steps were undertaken to identify and resolve the problem, including: (1) verifying temporal overlap between the electron beam and the laser using fast photodiode and oscilloscope measurements; (2) determining the precise beam energy by measuring the radiation spectrum; and (3) shortening the laser pulse duration from 18 ps to 2 ps.

Ultimately, it was discovered that the electron beam had been constantly aligned to the reflected laser beam, rather than the main laser. Further investigation revealed that the beam splitter in the screen camera setup had been installed incorrectly. After correcting the beam splitter orientation and realigning beams, clear slice energy modulation was observed, as shown in Fig. 8.

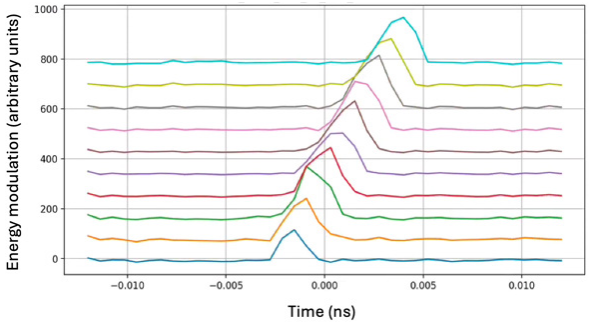

Figure 8: Observed energy modulation for different sliced beams.

Beam Halos

The injector bunch length is typically compressed by a factor of three using the buncher system only. However, beam halo has been intermittently observed on the injector screens. To address this, we implemented a two-stage bunch compression scheme: first, using the buncher, and then utilizing the second cavity of CM01 by setting its phase to the zero-crossing. This approach allows for gradual bunch compression, which helps beam transport to avoid dramatic changes to the beam optics, reducing the formation of beam halos. Experimental results confirm that this new scheme mitigates beam halo compared to the previous single-stage compression method.

We acknowledge T. Luo (LBNL) for the new cathode design, and LCLS-II commissioning team particularly A. Benwell, F. Decker, A. Fisher and J. May for the support of the work.

REFERENCES

[1] F. Zhou *et al.*, "Commissioning of the SLAC Linac Coherent Light Source II electron source", Phys. Rev. Accel. Beams, vol. 24, p. 073073401, 2021. doi:10.1103/PhysRevAccelBeams.24.073401

[2] T. Luo and D. Dowell, "Recent new cathode development for LCLS-II photoinjector", AD forum, SLAC, July 18, 2025.